MBoC | BRIEF REPORT

Mechanical strategies supporting growth and size diversity in Filamentous Fungi

Louis Chevalier[a,b,†], Flora Klingelschmitt[a,b], Ludovic Mousseron[a,b], and Nicolas Minc[a,b,*]
[a]Université Paris Cité, CNRS, Institut Jacques Monod, F-75013 Paris, France; [b]Equipe Labellisée LIGUE Contre le Cancer, 75013 Paris, France

ABSTRACT **The stereotypical tip growth of filamentous fungi supports their lifestyles and functions. It relies on the polarized remodeling and expansion of a protective elastic cell wall (CW) driven by large cytoplasmic turgor pressure. Remarkably, hyphal filament diameters and cell elongation rates can vary extensively among different fungi. To date, however, how fungal cell mechanics may be adapted to support these morphological diversities while ensuring surface integrity remains unknown. Here, we combined super-resolution imaging and deflation assays to measure local CW thickness, elasticity and turgor in a set of fungal species spread on the evolutionary tree that spans a large range in cell size and growth speeds. While CW elasticity exhibited dispersed values, presumably reflecting differences in CW composition, both thickness and turgor scaled in dose-dependence with cell diameter and growth speeds. Notably, larger cells exhibited thinner lateral CWs, and faster cells thinner apical CWs. Counterintuitively, turgor pressure was also inversely scaled with cell diameter and tip growth speed, challenging the idea that turgor is the primary factor dictating tip elongation rates. We propose that fast-growing cells with rapid CW turnover have evolved strategies based on a less turgid cytoplasm and thin walls to safeguard surface integrity and survival.**

Monitoring Editor
Sophie Martin
Université de Genève

Received: Apr 17, 2024
Revised: Jul 3, 2024
Accepted: Jul 11, 2024

Challenge
Cross-Species
New Hypothesis
Open Data

SIGNIFICANCE STATEMENT

- Filamentous fungi feature large variations in cell size and growth speeds but the mechanical underpinning supporting these variations are unknown.
- The authors provide measurements of turgor pressure, cell wall (CW) thickness and elasticity across several fungi to establish scaling laws coupling size, growth, and cell mechanical properties.
- This work provides an important resource of numbers on cell mechanics across species and sheds light on evolutionary strategies constraining cell morphology, mechanics, and survival.

This article was published online ahead of print in MBoC in Press (http://www.molbiolcell.org/cgi/doi/10.1091/mbc.E24-04-0171) on July 24, 2024.

†Present address: Université Côte d'Azur, CNRS, INSERM, Institute of Biology Valrose (iBV), 06108 Nice, France.

*Address correspondence to: Nicolas Minc (nicolas.minc@ijm.fr).

Abbreviations used: AFM, Atomic Force Microscopy; CW, Cell Wall; ConA, ConcanavalinA; GS-IB4, Griffonia simplicifolia – Isolectin B4; WGA, Wheat germ agglutinin.

INTRODUCTION

Survival is a fundamental constraint that shapes the evolution of living organisms. The survival, lifestyles and functions of many organisms, including bacteria, fungi and plants, are associated to the synthesis of a rigid cell wall (CW) that encases the plasma membrane to mechanically protect these cells. CWs are composed of diverse polysaccharides and proteins that largely vary among species and phyla. CWs are elastic and, as such, maintain cell shapes, but they also remodel locally to incorporate plastic deformation, a process key for cell growth (Lew, 2011; Municio-Diaz *et al*., 2022). Walled cells also feature a large internal cytoplasmic turgor pressure, which is osmotically generated and can reach values on the order of

several atmospheres (Money, 1990; Lew *et al.*, 2004; Beauzamy *et al.*, 2014). Turgor inflates the CW and puts it under tension, and is as such thought to be a key driving element to permit growth against fundamental forces including gravity and resistive forces from multiple substrates such as soils or host tissues (Bastmeyer *et al.*, 2002; Lew, 2011; Mishra *et al.*, 2022). In general, however, how walled cell mechanics may be fit to the function, morphology, or environment of different organisms remains poorly studied.

Filamentous fungi are ancient walled eukaryotes, which span ~600 Myears of evolution (Naranjo-Ortiz and Gabaldón, 2020; James *et al.*, 2006; Stajich *et al.*, 2009). They occupy most environments on earth and represent an important class of pathogens for animals and plants. A wide spread strategy adopted by fungi to colonize space, reproduce or infect their hosts is tip growth (Steinberg *et al.*, 2017). Tip growth implicates a highly polarized synthesis and remodeling of the CW at cell tips, in part regulated by the cytoskeleton and small GTPases like Cdc42 and Rac that restrict the secretion of synthesis and remodeling CW enzymes to cell tips (Martin and Arkowitz, 2014; Davi and Minc, 2015; Steinberg *et al.*, 2017; Municio-Diaz *et al.*, 2022). Interestingly, in spite of conserved mechanisms and effectors, tip growth and hyphal shapes feature a remarkable variability across species, with some fungi, like *Fusarium oxyparum*, that grow thin hyphae of less than 1 µm in diameter (Ruiz-Roldán *et al.*, 2010), up to very large cells found in *Neurospora crassa* or *Sclerotinia sclerotiorum* that may reach diameters as large as 10–20 µm (Fischer-Parton *et al.*, 2000). Tip growth speeds also span a remarkably large range of values, from relatively slow elongating yeast cells that grow at ~1 µm/h up to some of the fastest fungi that elongate as fast as 500 µm/h (López-Franco *et al.*, 1994; Taheraly *et al.*, 2020).

Variations in growth speeds and hyphal shapes may derive from the modulation of rates of CW synthesis and turnover and the size of polarity/secretion zones, respectively (Köhli *et al.*, 2008; Kelly and Nurse, 2011; Bonazzi *et al.*, 2015; Chevalier *et al.*, 2023). However, deformation of freshly assembled wall portions is also thought to require tensional stresses derived from turgor, as reducing turgor in most fungal cells halts growth in a near-instantaneous manner (Money, 1990; Minc *et al.*, 2009). Importantly, such tensional stresses also entail large risks of CW failure, with CW elastic strains at cell tips estimated to be around 20–30% and failure strains, at which the CW breaks open, measured to be around ~40–50% in some fungal species (Stenson *et al.*, 2011; Davi *et al.*, 2019). Accordingly, tip bursting is a common phenotype of fungal hyphae treated with a hypoosmotic medium to increase turgor pressure or of mutant cells defective in CW synthesis (Bartnicki-Garcia and Lippman, 1972; Davì *et al.*, 2018). To date, which mechanical strategies fungal cells may have employed to cope with the risks associated with rapid cell growth have not been tackled in a systematic manner. In part, progress in this fundamental question has been limited by the low throughput associated with typical methods like AFM, commonly used to measure CW mechanics and turgor, and that of electron microscopy to measure CW thickness. As such, only a few reports provide comparative measurements of cell mechanics among different species and strains (Davi *et al.*, 2019; Lemière and Chang, 2023).

Here, we adapted a sub-resolution microscopy method to image CW thickness (Davì *et al.*, 2018; Chevalier *et al.*, 2023) in live cells of seven fungal species selected among distant branches on the fungal evolutionary tree based on their differences in hyphal cell diameters and elongation speeds. We coupled thickness measurements to strain-stress assays based on CW elastic relaxation achieved by ablating CWs with a laser and/or the application of ranges of osmotic shocks (Atilgan *et al.*, 2015; Davi *et al.*, 2019). This allowed us to measure with medium throughput basal values of turgor pressure, CW thickness and elastic moduli. Our results reveal relatively dispersed values of elastic moduli both at cell tips and sides, plausibly reflecting differences in CW compositions across fungi. In contrast, both CW thickness and turgor appeared to inversely scale with cell size and tip growth. These findings suggest a counterintuitive scaling with rapid growing and large cells featuring less tensed CWs. We propose that this strategy may limit the risks of failure when CWs remodel rapidly.

RESULTS AND DISCUSSION

Mapping the mechanical properties in different fungal species

To analyze how CW mechanics and turgor may vary among fungal species that feature cells with different sizes and elongation speeds, we selected seven representative species across the fungal kingdom, namely *Neurospora crassa, Botrytis cinerea, Aspergillus nidulans, Penicilium janczewskii, Candida albicans, Schizosaccharomyces pombe and Mucor circinelloides* (Figure 1A; Supplemental Table S1). Measurements for *S. pombe* and *A. nidulans* were taken from our own previous studies employing the exact same strategy as described here (Davi *et al.*, 2019; Chevalier *et al.*, 2023). Among these species, six are septate fungi that belong to different clades of ascomycetes, and one, *Mucor circinelloides* is a more distant non-septate fungus. Also, several of these selected fungi are known opportunistic human pathogens (*Mucor circinelloides and Candida albicans*), and one is a plant pathogen (*Botrytis cinerea*). Species were selected based on morphological features, especially hyphal diameter and tip elongation speeds from previous reports, and also as relatively simple systems to grow in laboratory conditions (López-Franco *et al.*, 1994; Fischer-Parton *et al.*, 2000; Figure 1B). Importantly, hyphal cells were all imaged using similar microscopy setups, but media and temperature were adapted to the different species (Supplemental Table S1).

In order to measure CW thickness around live hyphae, we adapted a previous subresolution method developed in *S. pombe* and *A. nidulans*, based on the subpixel segmentation of the inner and outer faces of CWs, labelled with fluorophores of different colors (Davi *et al.*, 2019; Chevalier *et al.*, 2023). We labeled the outer face of CWs with either WGA, ConA or GS-IB4 lectins (depending on species) bound to far-red emitting fluorophores (Supplemental Figure S1; Supplemental Table S2). Membranes were labeled with integral or membrane-bound proteins in tractable species (*Schizosaccharomyces pombe*, *Aspergillus nidulans, Candida albicans* and *Neurospora crassa*; Vauchelles *et al.*, 2010; Davì *et al.*, 2018; Serrano *et al.*, 2018; Chevalier *et al.*, 2023), and by using the FM-4 64 dye in other species (Supplemental Figure S1; Supplemental Table S2; Fischer-Parton *et al.*, 2000). However, as this dye is rapidly endocytosed, cells were placed in open liquid chambers labeled with lectins, and FM-4 64 was added close to the field of view before immediate imaging. After imaging membranes and lectins, cells were rapidly pierced using a UV laser-focused on the cell surface. This caused cells to deflate and CWs to relax, from which we measured CW elastic strains (Atilgan *et al.*, 2015; Davi *et al.*, 2019). Assuming that the CW is homogenous, isotropic with a Poisson's ratio of 0, local thickness and elastic strains allowed to estimate local values of CW elastic moduli divided by pressure, Y/P, on cell sides or at cell tips (Abenza *et al.*, 2015; Atilgan *et al.*, 2015; Davi *et al.*, 2019). Finally, CW elastic strains measured from laser ablation were compared with elastic strains at different concentrations of sorbitol added to the medium, and media osmolarity was measured with an osmometer to estimate turgor values, *P* (Supplemental Figure S2; Atilgan *et al.*, 2015). Therefore, these methodologies allowed us to

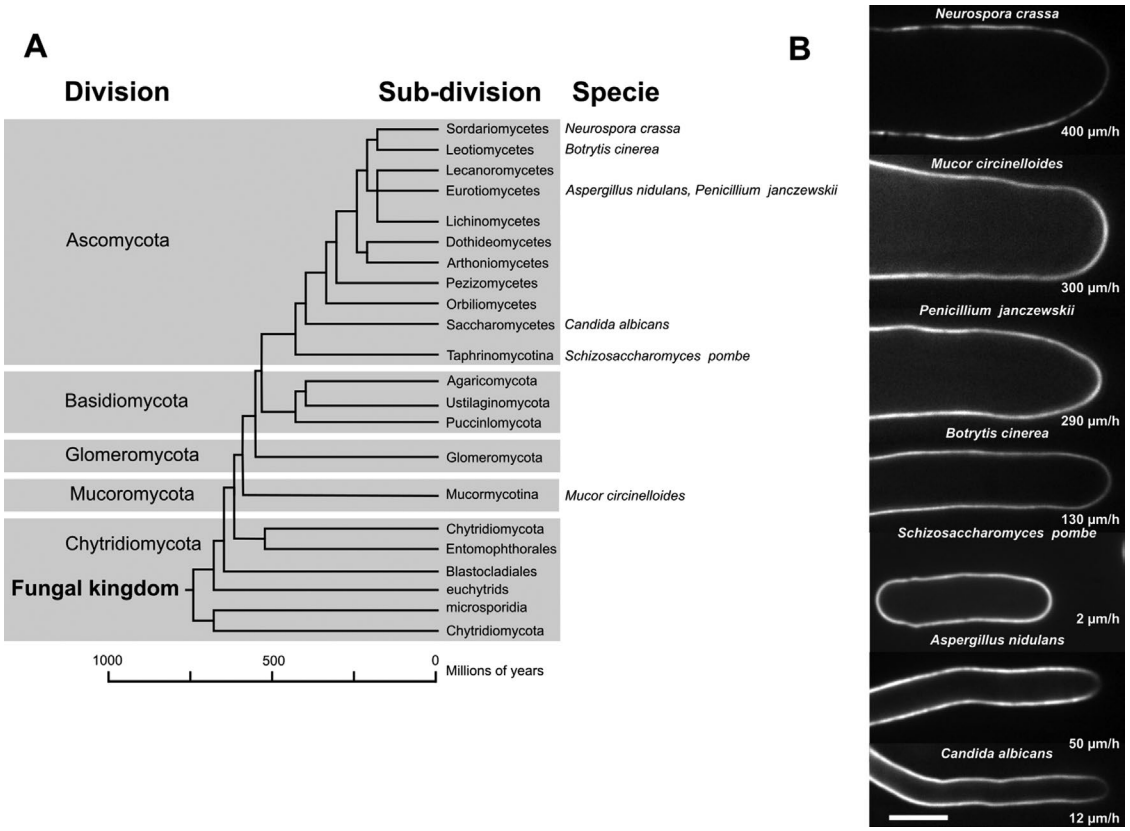

FIGURE 1: Diversity of size and speed across the fungal kingdom. (A) Phylogenetic tree showing fungal division, subdivision, and species used here. Adapted from refs. 44, 45. (B) Fluorescent confocal images of lectin signal to label the CW surface in the different used species, and their mean growth speed. Scale bar = 5 µm.

compute key local and global mechanical parameters at the single-cell level in multiple filamentous fungi (Figure 2A).

Scaling of cell mechanical parameters with hyphal cell diameter

We first explored putative correlations between cell radius, R, CW mechanical properties and turgor. In the fungi considered here, values of thicknesses of lateral CWs ranged from ~150–200 nm down to 30–50 nm, highlighting large variations among different species (Figure 2, B and C). Interestingly, lateral CW thickness values were generally smaller in wider cells for all the species considered, although we noted that *S. pombe* was above the general trend of other fungi. Importantly, the values measured agreed with thickness measurements from electron microscopy images found in the literature when available (Figure 2, B and C) (Bartnicki-Garcia and Nickerson, 1962; Trinci and Collinge, 1975; Zhao *et al.*, 2005; Davì *et al.*, 2018; Youssef *et al.*, 2019). In contrast, elastic Young's moduli that reflect bulk material properties of CWs and their polysaccharide composition and arrangements were more dispersed (Figure 2E). We interpret these variations as a plausible result of large variations in CW composition among fungi (Free, 2013; Gow *et al.*, 2017). CW surface moduli computed as the product of h and Y, which reflect an apparent stiffness for the CW, did not appear to increase with cell diameters and were also dispersed (Figure 2D). This suggests that wider lateral CWs are not necessarily stiffer among different fungal species. Strikingly, turgor values also showed clear dose-dependence variations with cell diameters, but surprisingly, wider cells appeared to feature a less turgid cytoplasm (Figure 2F). We conclude that fungal cells exhibit marked scaled variations in the mechanical properties of their lateral CWs as well as turgor values with their hyphal geometry, with wider cells having thinner walls and being less turgid.

To understand how these values may functionally affect the mechanical state of lateral CWs, we computed the circumferential CW tension (PR), stress (PR/h), elastic strain (PR/hY), and bending energy rescaled to that of pressure (PR^3/Yh^3; Supplemental Figure S3; Davi *et al.*, 2019). We note that the longitudinal counterparts of these parameters have a similar dependence on P, R, h or Y, but with a prefactor of ½. This analysis showed that the circumferential CW tension was generally lower in larger cells but did not reveal any simple scaling relationships for CW stress (Supplemental Figure S3, A and B). Rescaled bending energy values also increased progressively with cell diameter, suggesting that lateral CWs of wider cells found in different species may be easier to bend (Supplemental Figure S3D). Finally, with the exception of *Candida albicans,* which was above the general trend, the elastic strain of lateral CWs was mostly flat, at values around ~20%, raising the possibility that limitations in CW deformation may constrain cell diameter definition to ensure wall integrity. We conclude that wide fungal cells feature less pressurized cytoplasm and thinner lateral CWs, which contribute to limiting elastic strains in their lateral CWs.

Scaling of cell mechanical parameters with hyphal cell growth

Next, we focused on CW mechanical properties at cell tips to understand how they may be modulated as a function of hyphal cell elongation speeds. As previously reported, wider cells generally grew faster (López-Franco *et al.*, 1994), presumably reflecting a higher

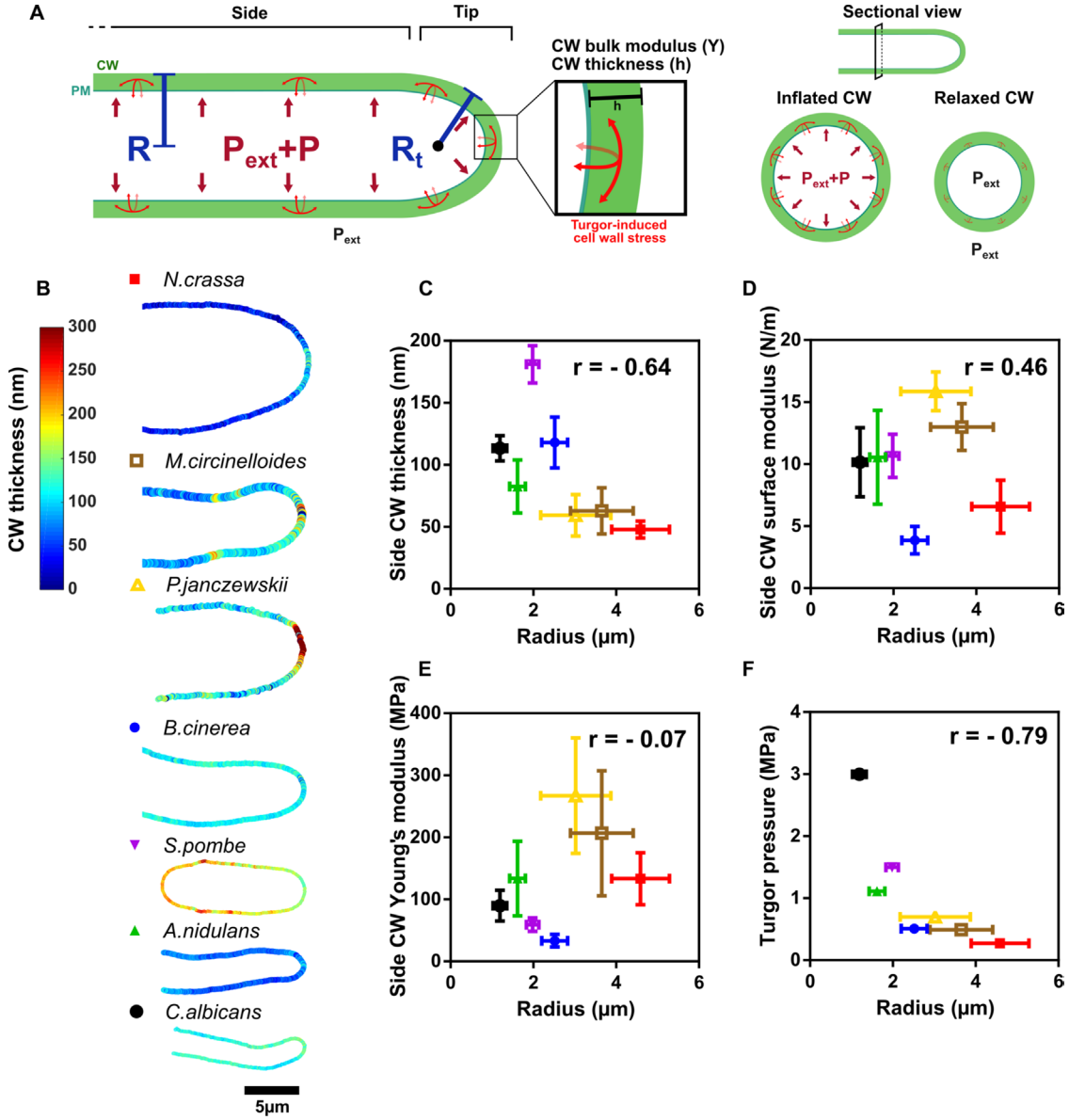

FIGURE 2: Cell mechanics and cell size in filamentous fungi. (A) Scheme of hyphal mechanics, representing the radius (R), the tip curvature radius (Rt), the turgor pressure (P), the cell wall thickness (h), and the CW Young's modulus (Y). Internal turgor pressure stretches elastically the CW. (B) Color maps of CW thickness for the different fungal species considered in this study. (C–F) Mechanical parameters of lateral CWs plotted against the cell radius. Side cell wall thickness ($n > 16$ cells for each species) (C), side CW Young's modulus ($n > 16$ for each species) (D), side CW surface modulus (($n > 11$ for each species) (E), and turgor pressure ($n > 15$ for each species) (F). Error bars correspond to ±SD. Indicated r values on the graphs are Pearson correlation coefficients. Scale bar = 5 µm.

CW remodeling activity at cell tips (Taheraly *et al.*, 2020; Figure 3A). Interestingly, we found that values of CW thickness at cell tips were inversely correlated with growth speeds, suggesting that rapidly growing cells feature thinner tip CWs (Figure 3B). In addition, the ratio of CW thickness between cell tips and cell sides also increased with tip growth speeds, with rapid species like *P. janczewskii*, *M. circinelloides*, and *N. crassa* that featured a thicker CW at cell tips as compared to cell sides, and relatively slower ones like *A. nidulans* and *S. pombe*, with the opposite CW thickness polarity (Figure 4A). Both CW Young's and surface elastic moduli at cell tips, exhibited dispersed values among different species as for lateral CWs (Figure 3, C and D). Yet, the ratio of both bulk and surface moduli between tips and lateral CWs was systematically below one, in agreement with the notion that the CW at cell tips is softer than on cell sides to promote anisotropic cell elongation (Figure 4, B and C; Mishra *et al.*, 2022). In addition, this ratio was smaller in ,faster-growing cells, indicating that the polarization of CW stiffness may become more pronounced as cells grow faster (Figure 4, B and C). Finally, one of the most unique and surprising features was the finding that faster-growing cells have lower turgor pressure values than slow-growing ones (Figure 3E). For instance, fission yeast turgor was measured to be around 1.5 MPa with cells elongating at ~2 µm/h and turgor in *N. crassa* was only ~0.2 MPa with cells growing at ~400 µm/h. Together, these findings suggest a counterintuitive scaling in which faster-growing cells feature thinner walls at their cell tips and a less turgid cytoplasm.

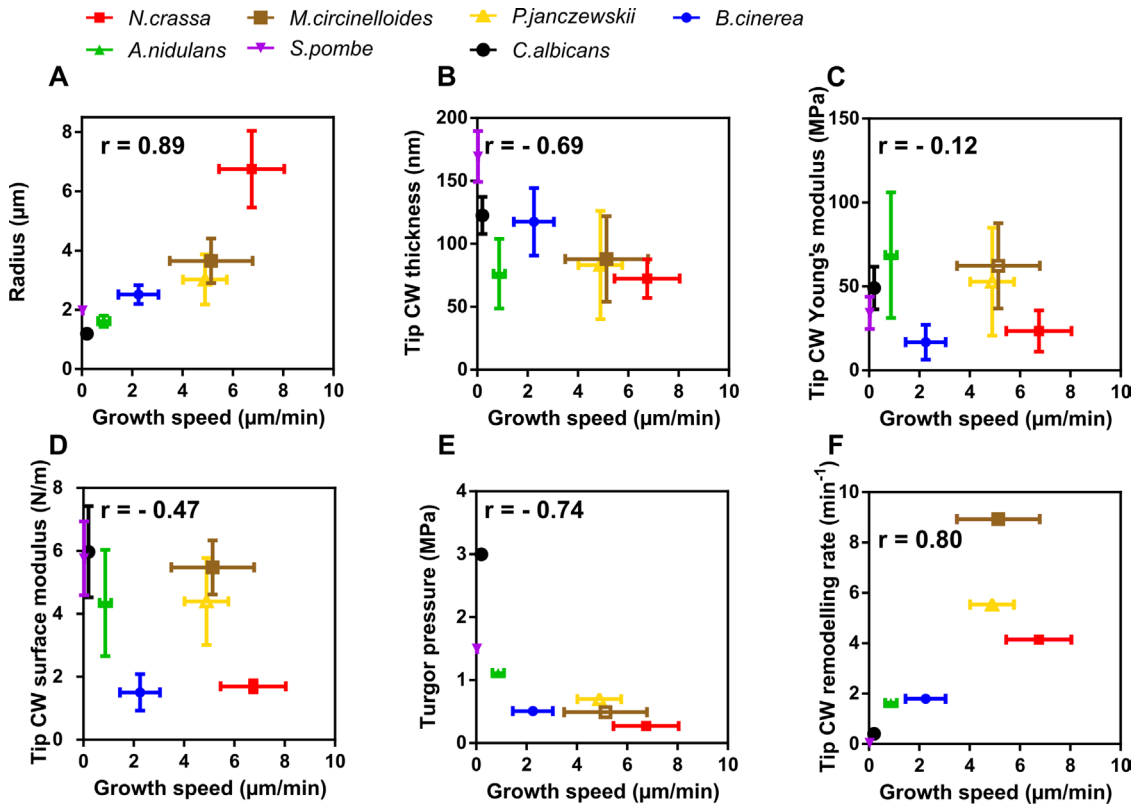

FIGURE 3: Apical mechanical parameters dependence on tip growth speed. Mechanical and geometrical parameters plotted against average growth speed for different fungal species. Radius ($n > 23$ cells for each species) (A), tip CW thickness ($n > 11$ for each species) (B), tip CW Young's modulus ($n > 11$ for each species) (C), tip CW surface modulus ($n > 7$ for each species) (D), pressure ($n > 15$ for each species) (E), and effective CW remodeling rate (F). The effective remodeling rate is calculated as the growth speed divided by PR^2/Yh. Error bars correspond to ±SD. Indicated *r* values on the graphs are Pearson correlation coefficients.

To understand whether these properties may arise from constraints in tip CW tension, stress, or elastic strains, we computed these parameters at cell tips by assuming a hemispherical geometry for all cell tips considered (Supplemental Figure S4). We found that CW tension at cell tips was negatively correlated with tip growth speeds, while CW stress did not show such a clear tendency (Supplemental Figure S4, A and B). The CW elastic strain was constant, around ~25% for most species and lower in some of the fastest cells (Supplemental Figure S4C). The rescaled bending energy of tip CWs exhibited a large diversity of values, with a positive correlation with growth speeds (Supplemental Figure S4D). Finally, previous modeling approaches have suggested that tip growth speed may depend on a product between an effective CW remodeling rate, *a*, and the elastic strain multiplied by the radius (PR^2/hY; Davì *et al.*, 2018). We, therefore, used our mechanical measurements to extract the value of *a* as a function of tip growth speeds and found that faster-growing cells may remodel their CWs much faster than slower ones and that this parameter could be the most variable effector of tip growth speeds (Figure 3F). Together, these results suggest that faster-growing cells exhibit less turgid cytoplasm thin apical walls but higher CW remodeling rates a strategy which may allow them to limit CW strains at cell tips and consequent risks of tip bursting.

In conclusion, we here implemented subresolution imaging and stress-strain measurements in a set of representative fungal species. These analyses allow for the computation of local thickness, bulk CW material properties, as well as turgor and should be applicable to other types of fungi, allowing to monitor cell mechanics in situations representative of infection phases or response to antifungal agents, for instance. As such, these data provide an important resource of fungal cell mechanical parameters that may impact our understanding of morphological variations found across species (Campàs *et al.*, 2012; Ohairwe *et al.*, 2024). We found that CW bulk material properties vary across fungi and are not necessarily scaled with cell size or growth speeds, which we interpret as a signature of variations in CW compositions or crosslinks across fungi (Free, 2013; Gow *et al.*, 2017). In contrast, CW thickness and turgor were inversely scaled with cell size and growth speeds, being both smaller in larger and more rapidly growing hyphae. This inverse scaling tended to limit CW tension and elastic strains both on lateral and apical CWs. As shown in most fungi, hypoosmotic treatments that effectively increase turgor most often cause large tip-bursting and lysis phenotypes (Bartnicki-Garcia and Lippman, 1972). Therefore, we propose that such mechanical scaling in filamentous fungi may arise from the selective pressure to limit CW elastic deformations and promote CW integrity. Another important plausible consequence of lowering turgor may also be at the level of membrane recycling. As shown in yeast, turgor opposes actin-based forces to set the rate of vesicle internalization (Basu *et al.*, 2014; Dmitrieff and Nédélec, 2015; Ma and Berro, 2021). As very rapid tip-growing cells employ faster recycling rates, we speculate that reducing turgor could also be a mechanical strategy to facilitate trafficking events such as endocytosis in these cells (Picco *et al.*, 2024). Interestingly, mechanical parameters did not seem to be phylogenetically constrained with, for instance, very distantly related fungi like

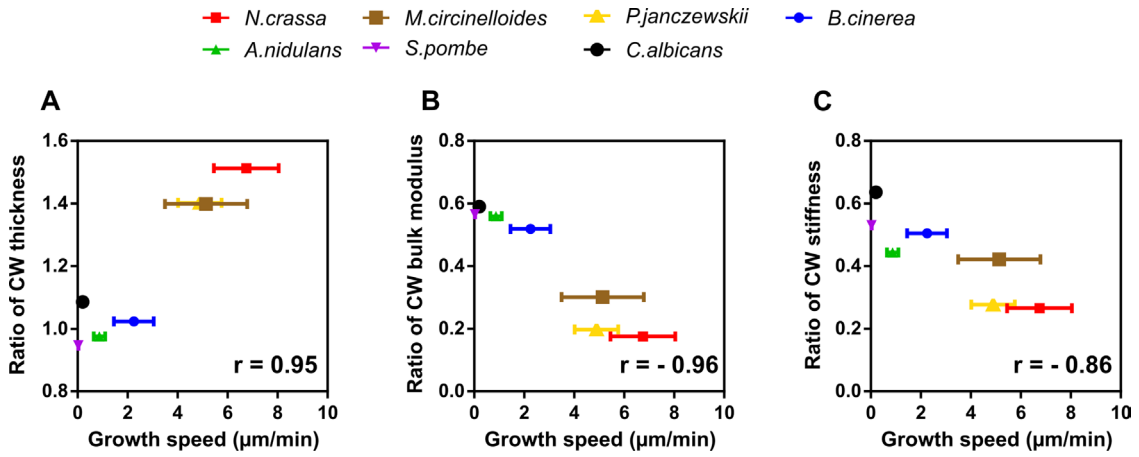

FIGURE 4: CW mechanical anisotropies and cell growth. Ratio of apical over lateral CW thickness (A), CW bulk modulus (B), and CW stiffness (C) plotted against mean growth speed. Error bars correspond to ±SD. Indicated *r* values on the graphs are Pearson correlation coefficients.

M. circinelloides and *N. crassa* featuring a similar range of values for both CW thickness and turgor pressure. This suggests that parameters such as turgor and CW thickness may have evolved relatively rapidly in the fungal tree to facilitate adaptation to different cell sizes and growth speeds. Future work coupling mechanical measurements with biochemical characterization of CWs and turgor regulation may help address how biomechanical and biochemical designs have coevolved to support morphogenetic diversity and survival.

MATERIAL AND METHODS

Request a protocol through *Bio-protocol*.

Fungal growth conditions and medium

Culture media were adapted to each species (see Supplemental Table S2). Cells were grown on either Vogel's medium (1.5% sucrose), MAE (2% malt and 2% glucose, 0.1% peptone), MCA (1% glucose and 5 mM ammonium tartrate), spider (1% nutrient broth and 1% mannitol), DO (2% glucose), or YE5S (3% glucose). Cultures were less than a day old, grown in liquid from spore solutions, using eight-well dishes (IBIDI GmbH, Martinriesd, Germany). *Candida albicans* was grown on liquid YPD (2% glucose), and cells in exponential growth were then harvested, rinsed, and placed in spider medium to induce filamentation, and experiments were only carried out on the hyphal form.

Membrane and CW labeling

The CW was labeled using either 10 µg/ml of WGA (Sigma, L9640) or 70 µg/ml of ConA (ThermoFisher, C21421), depending on the species (see Supplemental Table S2). For some nontractable fungi, the plasma membrane was labeled using FM4-64 (Thermo Fisher, T13320). To circumvent rapid endocytosis of the marker, droplets of ~1 µl of 1 µg/ml of FM4-64 were added close to the chosen hyphae, yielding a bright membrane signal, and the images were taken within less than a minute after dye addition.

Sorbitol treatments

Sorbitol shocks were done either in Ibidi wells or in PDMS chambers in which hyphal cells were maintained in the plane by being sandwiched in between dialysis membranes and cover glasses to constraint hyphae in two dimensions (Charvin *et al.*, 2008; Haupt *et al.*, 2018). Cells were grown overnight from spore cultures in 1 × 4 cm PDMS chamber or in ibidi wells. Next, cells were imaged, rinsed with a medium supplemented with sorbitol, and imaged again less than a minute later. For *Mucor circinelloides* and *Penicillium janczewskii* a single layer of dialysis membrane was positioned between cells and the roof of the PDMS in order to constrain hyphae to stay relatively flat and limit movements of hyphae after osmotic shocks.

For *N. crassa*, cells were grown on agar media for 1 d at 30°C in the dark and 1 d at 4°C. An agar square with front-line hyphae was then cut and placed in an ibidi chamber filled with liquid media (López-Franco *et al.*, 1994). After the hyphae reached the border of the agar zone, images were taken, medium supplemented with sorbitol was added, and the same hyphae were imaged.

Microscopy

Imaging was done at room temperature, using an inverted spinning-disk confocal microscope equipped with a motorized stage, automatic focus (Ti-Eclipse, Nikon, Japan), a Yokogawa CSUX1FW spinning unit, and a 100X oil-immersion objective (CFI Plan Apo DM 100X/1.4 NA, Nikon). We used either an EM-CCD camera (ImagEM-1K, Hamamatsu Photonics, Japan) with a 2.5X additional magnifying lens or a Prime BSI camera (Photometrics).

Laser ablation of the CW was done using a diffraction-limited spot from a 355-nm laser, with an iLas2 module (Gattaca, France) in the "Mosquito" mode, and performed on a 60X oil-immersion objective (CFI Apochromat 60X Oil lS, 1.4 NA, Nikon). Images were acquired with the 100X oil-immersion objective. The microscope was operated with the Metamorph software (Molecular Devices).

Tracking of cell shape during osmotic shocks was done using a Leica DMI6000 B microscope equipped with an A-Plan 40x/0.65 PH2 objective and an ORCA-Flash4.0LT Hamamatsu camera.

Image analysis

CW thickness analyses. CW thickness measurements were done according to previous work (Davì *et al.*, 2018; Chevalier *et al.*, 2023), using two-color mid-slice confocal images. Using an automated script, the positions of both signals were extracted by Gaussian fitting. Local distances between signals, which correspond to local values of CW thickness, were computed after chromatic shift and in/out signal correction.

Turgor pressure measurement. Turgor pressure was measured as in (Atilgan *et al.*, 2015; Chevalier *et al.*, 2023) by comparing the shrinkage of cells rinsed with media supplemented with sorbitol at

different concentrations (0–4 M) with the shrinkage obtained by photo-ablation of the CW. Shapes were compared before and less than a minute after the osmotic shock to limit osmoadaptation. Cell diameters were measured manually using Image J. The internal osmolyte concentration $\bar{C}_0$ was measured as:

$$\bar{C}_0 = C_0 + C_{mediun}$$

With C_0 the sorbitol concentration at which the cell shrinks as much as with photoablation and C_{mediun} the molarity of the medium used was measured using a vapor pressure osmometer (5600, Vapro Vapor Pressure Osmometer).

From this, we calculated the effective concentration of the cytoplasm in the normal state $\bar{C}_1$:

$$\bar{C}_1 = \bar{C}_0 \frac{\frac{V_0}{V_1} - \beta}{1 - \beta}$$

Where V_0 / V_1 is the ratio between the volume before and after ablation, and β the inaccessible volume fraction, taken to be 0.22 (Atilgan *et al.*, 2015).

This yields an estimate of turgor, *P*, from the relationship:

$$P = \left(\bar{C}_1 - C_{media}\right) RT$$

CW Young's modulus. The Young's modulus (Y) divided by pressure (P) was obtained by combining CW thickness measurement and photo-ablation assays. Assuming that the CW is homogenous and isotropic, with a Poisson's ratio of 0, the force balance in the cylindrical part yields:

$$\frac{Y_{side}}{P} = \frac{R_1}{h_{side} R_1}$$

Where (R_1) and (R_0) are lateral cell radii before and after photoablation respectively, and $R_1 = \frac{R_1 - R_0}{R_0}$, the elastic strain of the lateral CW.

For the hemispherical shape of tips, force balance leads to:

$$\frac{Y_{tip}}{P} = \frac{R_{t1}}{2 h_{tip} R_t}$$

With $R_{t1} = \frac{R_{t1} - R_{t0}}{R_{t0}}$ the elastic strain at cell tips, R_{t1} being the tip radius of curvature before ablation, and R_{t0} after. Importantly, these analytical formula were show previously to be valid for relatively long tubes through numerical simulations (Davi *et al.*, 2019).

ACKNOWLEDGMENTS

We thank F. Leclerc (U. Paris Cité), R. Arkowitz (U. Nice), M. Peñalva (U. Madrid), A. Fleissner (U. Braunschweig), J. Dupont (MNHN) and P. Bassereau (I. Curie) for sharing strains, material and protocols, as well as A. Boudaoud for discussion, and V. Davì for initial assays on this project. L.C. acknowledges the "École Doctorale LPI - Program Bettencourt" and a 4th year fellowship from the Fondation de la Recherche Médicale (no 13171). This work was supported by the Centre National de la Recherche Scientifique (CNRS), the Université Paris Cité, and grants from La Ligue Contre le Cancer (EL2021. LNCC/ NiM), the European Research Council (ERC CoG "Forcaster" no. 647073), and the Agence Nationale pour la Recherche (ANR, "CellWallSense" no. ANR-20-CE13-0003-02).

REFERENCES

Abenza JF, Couturier E, Dodgson J, Dickmann J, Chessel A, Dumais J, Carazo Salas RE (2015). Wall mechanics and exocytosis define the shape of growth domains in fission yeast. Nat Commun 6, 8400.

Atilgan E, Magidson V, Khodjakov A, Chang F (2015). Morphogenesis of the fission yeast cell through cell wall expansion. Curr Biol 25, 2150–2157.

Bartnicki-Garcia S, Lippman E (1972). The bursting tendency of hyphal tips of fungi: Presumptive evidence for a delicate balance between wall synthesis and wall lysis in apical growth. Microbiology 73, 487–500.

Bartnicki-Garcia S, Nickerson WJ (1962). Isolation, composition, and structure of cell walls of filamentous and yeast-like forms of Mucor rouxii. Biochim Biophys Acta 58, 102–119.

Bastmeyer M, Deising HB, Bechinger C (2002). Force exertion in fungal infection. Annu Rev Biophys Biomol Struct 31, 321–341.

Basu R, Munteanu EL, Chang F (2014). Role of turgor pressure in endocytosis in fission yeast. Mol Biol Cell 25, 679–687.

Beauzamy L, Nakayama N, Boudaoud A (2014). Flowers under pressure: ins and outs of turgor regulation in development. Ann Bot 114, 1517–1533.

Bonazzi D, Haupt A, Tanimoto H, Delacour D, Salort D, Minc N (2015). Actin-based transport adapts polarity domain size to local cellular curvature. Curr Biol 25, 2677–2683.

Campàs O, Rojas E, Dumais J, Mahadevan L (2012). Strategies for cell shape control in tip-growing cells. Am J Bot 99, 1577–1582.

Charvin G, Cross FR, Siggia ED (2008). A microfluidic device for temporally controlled gene expression and long-term fluorescent imaging in unperturbed dividing yeast cells. PLoS One 3, e1468.

Chevalier L, Pinar M, Borgne RL, Durieu C, Peñalva MA, Boudaoud A, Minc N (2023). Cell wall dynamics stabilize tip growth in a filamentous fungus. PLoS Biology 21, e3001981.

Davi V, Chevalier L, Guo H, Tanimoto H, Barrett K, Couturier E, Boudaoud A, Minc N (2019). Systematic mapping of cell wall mechanics in the regulation of cell morphogenesis. Proc Natl Acad Sci USA 116, 13833–13838.

Davi V, Minc N (2015). Mechanics and morphogenesis of fission yeast cells. Curr Opin Microbiol 28, 36–45.

Davì V, Tanimoto H, Ershov D, Haupt A, De Belly H, Le Borgne R, Couturier E, Boudaoud A, Minc N (2018). Mechanosensation dynamically coordinates polar growth and cell wall assembly to promote cell survival. Dev Cell 45, 170–182.e7.

Dmitrieff S, Nédélec F (2015). Membrane mechanics of endocytosis in cells with turgor. PLoS Comput Biol 11, e1004538.

Fischer-Parton S, Parton RM, Hickey PC, Dijksterhuis J, Atkinson HA, Read ND (2000). Confocal microscopy of FM4-64 as a tool for analysing endocytosis and vesicle trafficking in living fungal hyphae. J Microsc 198, 246–259.

Free SJ (2013). Fungal cell wall organization and biosynthesis. Adv Genet 81, 33–82.

Gow NAR, Latge J-P, Munro CA (2017). The fungal cell wall: Structure, biosynthesis, and function. Microbiol Spectr 5, 25.

Haupt A, Ershov D, Minc N (2018). A positive feedback between growth and polarity provides directional persistency and flexibility to the process of tip growth. Curr Biol 28, 3342–3351 e3.

James TY, Kauff F, Schoch CL, Matheny PB, Hofstetter V, Cox CJ, Celio G, Gueidan C, Fraker E, Miadlikowska J, *et al.* (2006). Reconstructing the early evolution of Fungi using a six-gene phylogeny. Nature 443, 818–822.

Kelly FD, Nurse P (2011). Spatial control of Cdc42 activation determines cell width in fission yeast. Mol Biol Cell 22, 3801–3811.

Köhli M, Galati V, Boudier K, Roberson RW, Philippsen P (2008). Growth-speed-correlated localization of exocyst and polarisome components in growth zones of Ashbya gossypii hyphal tips. J Cell Sci 121, 3878–3889.

Lemière J, Chang F (2023). Quantifying turgor pressure in budding and fission yeasts based upon osmotic properties. Mol Biol Cell 34, ar133.

Lew RR (2011). How does a hypha grow? The biophysics of pressurized growth in fungi. Nat Rev Microbiol 9, 509–518.

Lew RR, Levina NN, Walker SK, Garrill A (2004). Turgor regulation in hyphal organisms. Fungal Genet Biol 41, 1007–1015.

López-Franco R, Bartnicki-Garcia S, Bracker CE (1994). Pulsed growth of fungal hyphal tips. Proc Natl Acad Sci USA 91, 12228–12232.

Ma R, Berro J (2021). Endocytosis against high turgor pressure is made easier by partial coating and freely rotating base. Biophys J 120, 1625–1640.

Martin SG, Arkowitz RA (2014). Cell polarization in budding and fission yeasts. FEMS Microbiol Rev 38, 228–253.

Minc N, Boudaoud A, Chang F (2009). Mechanical forces of fission yeast growth. Curr Biol 19, 1096–1101.

Mishra R, Minc N, Peter M (2022). Cells under pressure: how yeast cells respond to mechanical forces. Trends Microbiol, 30, 495–510.

Money NP (1990). Measurement of hyphal turgor. Experimental Mycology 14, 416–425.
Municio-Diaz C, Muller E, Drevensek S, Fruleux A, Lorenzetti E, Boudaoud A, Minc N (2022). Mechanobiology of the cell wall – Insights from tip-growing plant and fungal cells. J Cell Sci 135, jcs259208.
Naranjo-Ortiz MA, Gabaldón T (2020). Fungal evolution: Cellular, genomic and metabolic complexity. Biol Rev Camb Philos Soc 95, 1198–1232.
Ohairwe ME, Živanović BD, Rojas ER (2024). A fitness landscape instability governs the morphological diversity of tip-growing cells. Cell Rep 43, 113961.
Picco A, Toret CP, Rivier-Cordey A-S, Kaksonen M (2024). An evolutionary cell biology perspective into the diverging mechanisms of clathrin-mediated endocytosis in dikarya fungi. bioRxiv, https://doi.org/10.1101/2024.03.28.587219.
Ruiz-Roldán MC, Köhli M, Roncero MIG, Philippsen P, Di Pietro A, Espeso EA (2010). Nuclear dynamics during germination, conidiation, and hyphal fusion of *Fusarium oxysporum*. Eukaryot Cell 9, 1216–1224.
Serrano A, Illgen J, Brandt U, Thieme N, Letz A, Lichius A, Read ND, Fleißner A (2018). Spatiotemporal MAPK dynamics mediate cell behavior coordination during fungal somatic cell fusion. J Cell Sci 131, jcs213462.
Stajich JE, Berbee ML, Blackwell M, Hibbett DS, James TY, Spatafora JW, Taylor JW (2009). The fungi. Curr Biol 19, R840–R845.
Steinberg G, Penalva MA, Riquelme M, Wosten HA, Harris SD (2017). Cell biology of hyphal growth. Microbiol Spectr 5, 34.
Stenson JD, Hartley P, Wang C, Thomas CR (2011). Determining the mechanical properties of yeast cell walls. Biotechnol Prog 27, 505–512.
Taheraly S, Ershov D, Dmitrieff S, Minc N (2020). An image analysis method to survey the dynamics of polar protein abundance in the regulation of tip growth. J Cell Sci 133, jcs252064.
Trinci AP, Collinge AJ (1975). Hyphal wall growth in *Neurospora crassa* and *Geotrichum candidum*. J Gen Microbiol 91, 355–361.
Vauchelles R, Stalder D, Botton T, Arkowitz RA, Bassilana M (2010). Rac1 dynamics in the human opportunistic fungal pathogen *Candida albicans*. PLoS ONE 5, e15400.
Youssef K, Roberto SR, de Oliveira AG (2019). Ultra-structural alterations in *Botrytis cinerea*—The causal agent of gray mold—Treated with salt solutions. Biomolecules 9, 582.
Zhao L, Schaefer D, Xu H, Modi SJ, LaCourse WR, Marten MR (2005). Elastic properties of the cell wall of *Aspergillus nidulans* studied with atomic force microscopy. Biotechnol Prog 21, 292–299.